J Exp Clin Med 2010;2(5):231–238

ELSEVIER

ORIGINAL ARTICLE

Screening of Ethylnitrosourea Mice With Fatty Acid Oxidation Disorders by a Candidate Gene Approach After Proteome Analysis

Chun-Kuang Shih[1], Chiao-Ming Chen[2], Yi-Chun Chen[1], Hsiao-Chen Huang[1], Yuang-Tsong Chen[3,4], Sing-Chung Li[1]*

[1]*School of Nutrition and Health Sciences, Taipei Medical University, Taipei, Taiwan*
[2]*Department of Food Science, Nutrition and Nutraceutical Biotechnology, Shih Chien University, Taipei, Taiwan*
[3]*Institute of Biomedical Science, Academia Sinica, Taipei, Taiwan*
[4]*Duke University Medical Center, Durham, North Carolina, USA*

Received: Feb 9, 2010
Revised: Jun 6, 2010
Accepted: Jul 13, 2010

KEY WORDS:
ENU mice;
proteomic;
short chain fatty acid

Background/Purpose: Ethylnitrosourea (ENU) is an alkylating agent and primarily induces point mutations such as AT to TA transversions and AT to GC transitions. Due to its high mutagenicity, ENU mouse mutagenesis enables the generation and identification of mouse mutants with aberrance in various phenotypes and to identify novel genes relevant for the expression of the phenotype. The purpose of this study was to investigate the candidate genes involved in fatty acid oxidation disorders by the proteomic approach.
Methods: We screened ENU mice from 39 families from previously published data and identified two mutant mice that had a striking elevation in blood C4-OH short chain fatty acids compared with ENU controls. Total mitochondrial proteins were extracted from the gastrocnemius for two-dimensional electrophoresis, and two downregulated proteins, adenylate kinase isoenzyme 1 (AK1) and adenosine-5′-triphosphate (ATP) synthase D chain (ATP5H), were identified in the mutant mice through matrix-assisted laser desorption/ionization time-of-flight mass spectrometry.
Results: After genomic polymerase chain reaction and direct sequencing of *Ak1* and *Atp5h*, no variation was found in both gene sequence analyses.
Conclusion: Proteomic profiling can be a useful approach for detecting dynamic protein expression in ENU-induced mice. It is important to further clarify mechanisms of the mutant C4-OH disorder responsible for this expression.

1. Introduction

Ethylnitrosourea (ENU) is an alkylating agent that primarily induces point mutations. The most common mutations induced by ENU are AT to TA transversions and AT to GC transitions.[1,2] Because of its high mutagenicity, ENU can serve as a mouse model compound to explore the effect of factors such as dose response, dose fractionation, sex, and cell stage on the mutagenic action of chemicals[3,4] and as a model for disease treatments such as gene therapy and identifying novel genes.[5] ENU can transfer its ethyl group to oxygen or nitrogen radicals in DNA, resulting in mispairing and base-pair substitution if not repaired.[6] The molecular genetic data obtained from ENU-induced mutants on various species suggest that ENU produces mainly GC-AT transitions and, to a small extent, AT-GC, AT-CG, AT-TA, GC-CG and GC-TA base substitutions.[7]

*Corresponding author. School of Nutrition and Health Sciences, Taipei Medical University, 250 Wu-Hsing Street, Taipei 110, Taiwan.
E-mail: sinchung@tmu.edu.tw

More recently, the application of the global or proteomics approach to understanding tissue-specific disorders has been useful in identifying defective metabolic pathways.[8,9] The proteomic technology of two-dimensional gel electrophoresis (2-DE) is widely used in chickens,[10] pigs,[11] rats,[8,12,13] rabbits,[14] and humans,[15–17] and 2-DE remains the only technique that can be routinely applied to parallel quantitative expression profiling of large sets of complex protein mixtures.[18] Proteomic analysis of biological samples in disease models or therapeutic intervention studies is used to detect and identify biological proteins.[19] However, the technique has limited capability in resolving very small, very large, or highly basic, acidic, or hydrophobic proteins.[20]

β-oxidation of fatty acids is an important metabolic process that occurs in various organisms, ranging from bacteria to higher eukaryotes.[21] In mammals, two distinct β-oxidation systems exist, mitochondrial and peroxisomal. Mitochondrial β-oxidation provides acetyl groups that can be degraded to CO_2 and H_2O for the production of adenosine-5′-triphosphate (ATP), and is tightly coupled to the mitochondrial respiratory chain.[22] Mitochondrial fatty acid oxidation disorders are a group of clinically and biochemically heterogeneous inherited metabolic defects. The spectrum of phenotypes has expanded from hepatic encephalopathy to encompass myopathy, cardiomyopathy, peripheral neuropathy, sudden death and pregnancy complicated by fetal fatty acid oxidation disorders.[22]

We previously reported ENU mice with mitochondrial branched-chain aminotransferase deficiency resembling human maple syrup urine disease.[23] The limited fatty acid metabolic pathway could not resolve the C4-OH mice due to ENU mutation. To the best of our knowledge, proteomic profiling for detection of metabolic proteins of C4-OH mice has not been previously reported in mice or other animal models. Thus, we further investigated the molecular and cellular events characterizing the changes that occur in skeletal muscle of mice with an abnormal defect of short chain fatty acids. We carried out a combined genomic/proteomic approach to unravel the mutation in the protein expression profiles of the mutant mice.

2. Methods

2.1. Generation of ENU-recessive mice

ENU-treated mice were bred according to the three-generation breeding scheme as previously described[24] and were provided by the Institute of Biomedical Science, Academia Sinica[23] in Taipei, Taiwan. Briefly, C57BL/6J male mice were given three ENU intraperitoneal injections (100 mg/kg body weight) to generate G0 mice. G0 mice were then mated with normal B6 females to generate G1 male founder mice. Normal B6 females were mated with G1 male founders to generate G2 mice. G2 females were then backcrossed to G1 male mice to generate G3 offspring. Breeding and housing of the mice were conducted in the Mouse Mutagenesis Program Core Facility of Academia Sinica under specific pathogen-free conditions. The animal protocol was approved by the Institutional Animal Safety Committee. Mice were maintained on regular rodent diet (PicoLab Mouse Diet 20, product code 5058; Purina Mills Inc., Brentwood, Missouri, USA).

2.2. Blood organic acids analysis

We collected 100 μL whole blood from the mouse tail vein. The blood samples were diluted to 1 mL, derivatized with ethoxyamine hydrochloride at pH 10, acidified to pH 1, and then extracted four times with ethyl acetate (2 mL). After evaporation of the combined extracts, the residue was silylated with 100 μL of N, O-bis (trimethylsilyl) trifluoroacetamide with 1% trimethylchlorosilane plus 10 μL pyridine and analyzed by capillary column gas chromatography, using analytical conditions described previously.[25]

2.3. Mitochondrial protein extraction

To preserve the mitochondrial fraction, all procedures were performed at 4°C. Total mitochondrial protein was extracted from muscle tissue by a commercial mitochondria isolation kit (Sigma, St Louis, MO, USA) with some modification. One hundred mg of gastrocnemius muscle were excised and washed with cold extraction buffer (20 mM MOPS pH 7.5, 110 mM KCl, 1 mM EGTA, and 0.1 mM PMSF) twice. The tissue pellet was then resuspended with 10 volumes of extraction buffer containing 0.25 mg/mL trypsin, incubated on ice for 3 minutes and then the tissue was spun down a few seconds in a centrifuge. The supernatant was removed by aspiration, and eight volumes of the extraction buffer containing 0.25 mg/mL trypsin were added and then incubated on ice for 20 minutes. Albumin solution to 10 mg/mL was added to quench the proteolytic reaction, and then the tissue was mixed and spun down for a few seconds in a centrifuge. The supernatant was removed by aspiration and the mitochondrial pellet was washed three times with cold extraction buffer, and further homogenized using a homogenizer powered by an electric motor to ensure whole protein extraction. After centrifugation, the mitochondrial protein fraction was suspended in 2-D lysis buffer (7 M urea, 2 M thiourea, 4% CHAPS, 1% dithiothreitol, and 10 mM spermine), using an ultrasonic sonicator (Ultrasonic Liquid Processor; Sonaer Inc., Farmingdale, NY, USA), and assessed for protein concentration by an RCDC commercial kit (BIO-RAD, Hercules, CA, USA). The aliquots of mitochondrial protein were stored at –80°C for later 2-D analysis.

2.4. Two-dimensional gel electrophoresis

One hundred micrograms of mitochondrial protein were used in first dimension isoelectric focusing (IEF) carried out using the IPGphor system (GE Healthcare, Bethesda, MD, USA). Precast (18 cm, pH 4–7 or pH 3–10) immobilized pH gradient (IPG) dry strips were rehydrated overnight with 340 uL of buffer containing 8 M urea, 4% CHAPS, 20 mM DTT, and 2% IPG buffer (pH 4–7 or pH 3–10) and bromophenol blue. For analytical separations, the proteins were included in the rehydration buffer and IEF proceeded for up to 60,000 Vhr. For micro preparative separations, 300 μg of protein were used and focusing was extended to 100,000 Vhr in IPG strips by the IPGphor IEF System at 20°C. After one-dimensional isoelectrofocusing, the gel strips were equilibrated for 20 minutes in equilibration buffers [50 mM Tris-HCl, pH 8.8, 6 M urea, 30% glycerol, 2% sodium dodecyl sulfate (SDS), and 1% dithiothreitol], and then equilibrated for another 20 minutes in the same buffer containing iodoacetamide (5%, w/v). The second dimension separation was performed using a 10% SDS-polyacrylamide gel according to the Protean II XL vertical electrophoresis cells operating manual (BIO-RAD).

The IPG strip was placed on the surface of the second-dimension gel, and then sealed with 0.5% agarose in SDS-electrophoresis buffer (25 mM Tris base, 192 mM glycine, and 0.1% SDS). Electrophoresis was run overnight at 15°C at 24 mA per gel, and analytical gels were silver stained and gel images were acquired with a laser image scanner.

2.5. Gel staining, image analysis and spot selection

The preparative gel was stained using PhastGel Blue R (GE Healthcare). Digitized images of 2-D gels were generated using an ImageScanner II densitometer (Amersham Biosciences Corp., Piscataway, NJ, USA) and analyzed by ImageMaster 2-D Platinum 7 software (GE Healthcare). The volume for each spot on a gel was normalized against the volume of the total valid spots on the gel using the auto-normalization function of the ImageMaster 2-D software. Significantly differentially expressed protein spots ($p < 0.05$) with a twofold increase or decreased volume between controls and the ENU group were selected and cut from gels for protein identification.

2.6. Matrix-assisted laser desorption/ionization time-of-flight mass spectrometry (MALDI-TOF MS) identification

Briefly, protein spots cut from gels were destained with a solution of 15 mM potassium ferricyanide and 50 mM sodium thiosulfate (1:1), washed twice with deionized water and dehydrated in acetonitrile. The samples were then rehydrated in digestion buffer (20 mM ammonium bicarbonate and 12.5 ng/mL trypsin) at 4°C. After 30 minutes of incubation, the gels were digested for at least 12 hours at 37°C. The peptide solution was extracted twice using 0.1% trifluoroacetic acid in 50% acetonitrile and dried with N2. MALDI-TOF MS analysis was carried out on an ABI 4700 Proteomics Analyzer with delayed ion extraction (Applied Biosystems, Foster City, CA, USA). Mass spectra were obtained in a mass range of 700–3200 Da, using a laser (355 nm, 200 Hz) as the desorption ionization source. For MS/MS, the five precursor ions with the highest intensity were automatically selected to be analyzed. MS/MS accuracy was calibrated against the MS/MS fragments of m/z 1606.85, one of the peaks generated in myoglobin proton motive force. The parameters for peak matching were: minimum S/N, 20; mass tolerance, 0.2 Da; minimum peaks to match reference masses was four and the maximum outlier error was set to 100 ppm. Two thousand shots were used for each MS spectrum, while 3000 shots were used for MS/MS. The potential of mean force and MS/MS data collected were submitted as a combined search to MASCOT (Matrix Science Ltd., London, UK) using GSP Explorer software, V3.5 (Applied Biosystems) against the NCBI databases. Carbamidomethylation of cysteines and oxidation of methionines were the allowed peptide differential modifications. The maximum number of missed cleavages was set to one with trypsin as the protease. Protein homology identifications of the top hit (first rank) with a relative score exceeding a 95% probability and additional hits (second rank or more) with a relative score exceeding a 98% probability threshold were retained. The probability-based score, assuming that the observed match was significant ($p < 0.05$), had to be more than 50 (protein score) when submitting proton motive force data to the database, and be more than 30 (ion score) for individual peptide ions when submitting peptide sequence spectra. Every excised spot was performed in triplicate for protein identification.

2.7. Genomic polymerase chain reaction (PCR) and DNA sequencing

Genomic DNA was purified from the tail using the Puregene DNA purification kit (Gentra Systems, Minneapolis, MN, USA). All exons of candidate genes (*Ak1*, *Atp5h*) were amplified and sequenced. Primers were designed by the Primer3 PCR primer picking program (http://www-genome.wi.mit.edu/cgi-bin/primer/primer3_www.cgi) and previous published studies with some modifications.[26] The PCRs were performed in a final volume of 50 μL, containing 0.2 mM of each primer, 10 mM Tris-HCl (pH 8.3), 50 mM KCl, 1.5 mM $MgCl_2$, 0.2 mM dNTPs, 50 ng genomic DNA and 1 U TaKaRa Taq (Takara Bio Inc., Shiga, Japan). Amplification conditions consisted of an initial denaturation of 3 minutes at

95°C, followed by 20 cycles of touchdown PCR in 30 seconds at 95°C, 30 seconds at 65°C (decrease of 0.5°C per cycle), 40 seconds at 72°C; and a final 20 cycles in 30 seconds at 95°C, 30 seconds at 55°C, and 40 seconds at 72°C. All amplified PCR fragments were digested with shrimp alkaline phosphatase and ExoI to remove unincorporated primers and were sequenced using the BigDye Terminator Cycle Sequencing Kit v1.1/3.1 (Applied Biosystems) following the manufacturer's instructions. Sequencing products were separated on either an ABI Prism 3100 Genetic Analyzer or ABI PRISM 3700 DNA Analyzer and raw sequencing data were analyzed by the DNA Sequencing Analysis Software v3.7 (Applied Biosystems).

2.8. Statistical analysis

All experiments were conducted in triplicate. Results were reported as mean ± standard deviation. Paired *t* tests were performed to evaluate differences in parameters between control and ENU affected mice. A value of $p = 0.05$ was considered significant.

3. Results

3.1. Mutant mice with an abnormal short chain fatty acid pattern

In screening 614 G3 mice from 39 families from previously published data,[23] we identified two mutant mice that had a striking elevation of blood C4-OH short chain fatty acids (10-fold) compared with controls (Table 1). In addition, there was an abnormal fatty acid profile in the second sample of the same mouse obtained from 48 hours of fasting, and C4-OH expression was also elevated eightfold in mutants compared with controls. Subsequently, we also identified the second mouse in the same family as having an eightfold elevation in C4-OH expression and a sevenfold elevation in C4-OH expression after 48 hours of fasting compared with controls (Table 1). These similar abnormal fatty acid profiles in mutant mice in independent litters of the same family suggested that this phenotype was heritable. In addition, all mice had normal medium chain and long chain fatty acid profiles as well as amino acid profiles (data not shown).

3.2. Clinical phenotypes and C4-OH elevation

In addition to the abnormal C4-OH fatty acid profile, the mutant mice (1 male and 1 female) displayed a normal body weight, normal colored hair and there was no weakness or decreased spontaneous movement compared with unaffected siblings. A family history showed that although the mutant mice had increased C4-OH levels, the fertility rate and eating behavior were normal. None of the mice died prior to weaning or prior to metabolic screening at the newborn stage. After 2 years of feeding in the animal core facility, these C4-OH mice did not show any difference in phenotype compared with normal controls. Since the most striking fatty acid elevations were in C4-OH, and all short chain fatty acids share common metabolic pathways, we focused our investigations on C4-OH. The candidate genes involved in β-oxidation were screened and sequenced in the Institute of Biomedical Science of Academia Sinica; however, no variation was found by genome typing (data not shown).

3.3. Mitochondrial proteomic analysis and identification

Mitochondrial protein concentrations are approximately 10–20 mg/mL in muscle, and both control and C4-OH mice group were within the acceptable range. In both groups, the majority of protein bands were expressed equally in muscle mitochondrial protein by one-dimensional gel electrophoresis (data not shown). However, a further approach by 2-DE found that six

Table 1 Blood acylcarnitine concentrations in ethylnitrosourea (ENU) mutant and control mice*†

	Acylcarnitine concentrations (μM)				
	C3	C4	C4-OH	C5	C5-OH
Mouse					
ENU control ($n = 328$)	0.89 ± 0.36	0.28 ± 0.07	0.10 ± 0.04	0.20 ± 0.08	0.28 ± 0.09
Mutant 1	0.65 ± 0.18	0.22 ± 0.04	0.96 ± 0.03	0.15 ± 0.03	0.15 ± 0.03
Mutant 2	0.64 ± 0.19	0.26 ± 0.06	0.76 ± 0.11	0.13 ± 0.02	0.13 ± 0.02
After 48 hr fasting					
ENU control ($n = 10$)	0.81 ± 0.13	0.19 ± 0.06	0.16 ± 0.02	0.23 ± 0.04	0.29 ± 0.04
Mutant 1	0.89 ± 0.37	0.21 ± 0.13	1.26 ± 0.27	0.17 ± 0.07	0.27 ± 0.06
Mutant 2	0.95 ± 0.13	0.31 ± 0.09	1.12 ± 0.36	0.16 ± 0.04	0.32 ± 0.11

*One hundred μL whole blood from the mouse tail vein was prepared and analyzed by gas chromatography; †data are presented as mean ± standard deviation.

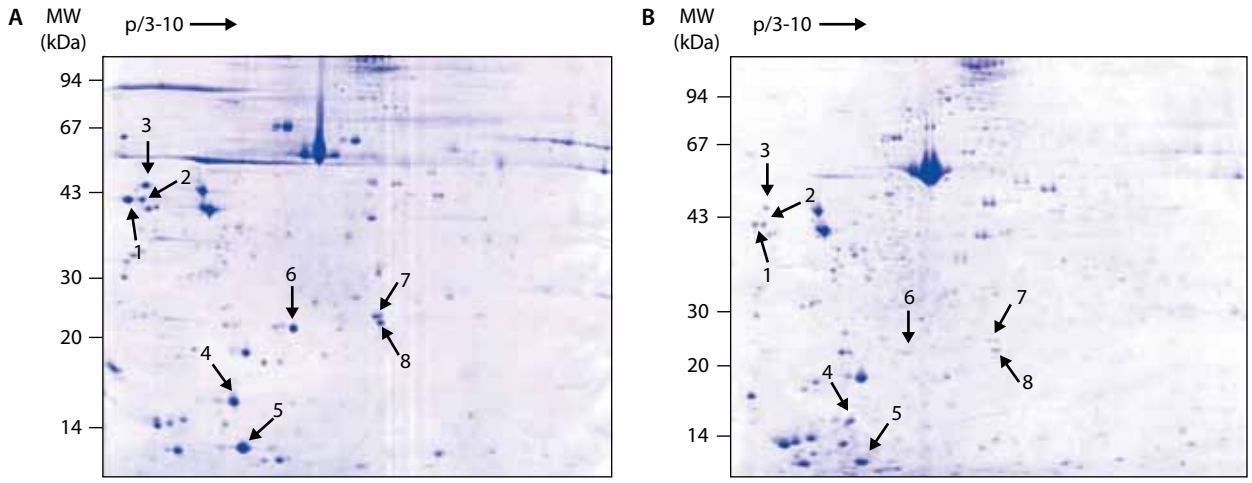

Figure 1 Two-dimensional analysis of mitochondrial proteins from normal and ethylnitrosourea mice. The mitochondria were extracted from gastrocnemius muscle by a commercial kit: (A) ethylnitrosourea control; (B) affected. Experiments were carried out in triplicate.

Table 2 Mitochondrial protein identification and quantification of ethylnitrosourea (ENU) control and C4-OH mice

Spot no.	Gene name	Description	Accession no.	Experimental *pI*/Mw (kD)	Fold change
1	Calsequestrin-1	Calcium-binding protein	O09165 (CASQ1_MOUSE)	3.9/45.6	5.2
2	Calsequestrin-1	Calcium-binding protein	O09165 (CASQ1_MOUSE)	3.9/45.6	2.4
3	Calsequestrin-1	Calcium-binding protein	O09165 (CASQ1_MOUSE)	3.9/45.6	2.7
4	Myosin light chain 2	This chain binds calcium	P97457 (MLRS_MOUSE)	4.8/18.9	2.2
5	Myosin light chain 3	Regulatory light chain of myosin	P05978 (MLE3_MOUSE)	4.6/16.6	1.5
6	Myosin light chain 6B	Regulatory light chain of myosin	Q8CI43 (MYL6B_MOUSE)	5.4/22.5	3.2
7	Adenylate kinase isoenzyme 1	Catalyzes the reversible transfer of the terminal phosphate group between ATP and AMP	Q9R0Y5 (KAD1_MOUSE)	5.7/21.5	4
8	ATP synthase D chain	Mitochondrial membrane ATP synthase	Q9DCX2 (ATP5H_MOUSE)	5.6/18.6	2.1

Differential spots were identified through matrix-assisted laser desorption/ionization time-of-flight mass spectrometry and data were evaluated in the MASCOT and NCBI databases. ATP = adenosine triphosphate; AMP = adenosine monophosphate.

proteins were upregulated in control mice (Figure 1). These six proteins were cut from gels for further identification by mass analysis. All identified proteins including calsequestrin-1, myosin light chain 2, myosin light chain 3, myosin light chain 6B, adenylate kinase isoenzyme 1 (AK1) and ATP synthase D chain (ATP5H) were 1.5-fold to 5.2-fold higher than in normal mice (Table 2). Because they mimic proteins in fatty acid metabolism, AK1 and ATP5H were chosen as candidate mutant proteins for causing C4-OH mice.

3.4. Genomic PCR and DNA analysis of *Ak1* and *Atp5h*

The genomic DNA was purified from normal and C4-OH affected mice tails. The quality of extracted DNA was examined by agarose gel electrophoresis and ethidium bromide staining, and the concentrations were evaluated by OD260 divided by OD280. Only qualified and completed genomic DNA was included for genomic DNA analysis. There are seven exons in both *Ak1* and *Atp5h*. DNA extracted from the C4-OH mouse tail in *Ak1* and *Atp5h* assays was of sufficient quality for PCR amplification; however, we did not find any sequence mutation in *Ak1 and Atp5h* (data not shown).

4. Discussion

When C4 levels are elevated in blood, hemoglobin and albumin, this causes an increased production of all C2–C6 fatty acids, with the most pronounced increase (4-fold) in C4–C6 fatty acids.[27] However, little is known about the new type of C4-OH. Investigation of our mutant mice did not lead to any clinical and laboratory findings resembling human short chain fatty acid

Please provide the citation for Table 3

Table 3 Primer set and polymerase chain reaction (PCR) product size of *Ak1* and *Atp5h*

Primer name	Sequence	PCR product size
Ak1-ex1-F	GTCAGCTGGGACCGGTTACT	434
Ak1-ex1-R	GAGAGTGGGGGAGGGATAGA	
Ak1-ex2-F	GGTGACAGAGGCAGGAGAAG	401
Ak1-ex2-R	AGCTCTGGGGTTCCAGAAAC	
Ak1-ex3-F	ACTCAAGGCGCCCATCTCT	436
Ak1-ex3-R	TTTCAGGACAGCCAGAACTATG	
Ak1-ex4-F	CTCTCATTGAGGACCGTGGT	443
Ak1-ex4-R	GAAGGGGCCACTCCAGTATT	
Ak1-ex5-F	GAAAGGGGTTTGCTGAAGC	429
Ak1-ex5-R	GACAAGCCCCACAGGATAAA	
Ak1-ex6-F	TTTTGGGCTTCCTCTTGAAA	467
Ak1-ex6-R	CACACAGCCCCAACTCAGTA	
Ak1-ex7-F	GCGCCTCTCTTTTCTAGCTG	400
Ak1-ex7-R	GAAGCAAAGGAAAGGAGCAA	
Atp5h-ex1-F	CCTTCCAGGACGGGACTC	312
Atp5h-ex1-R	AAAGCGAGCAGGGCAAAG	
Atp5h-ex2-F	CAACCAGCGCTAGAGATGAA	408
Atp5h-ex2-R	TCATCCTGTCCACAGCACAC	
Atp5h-ex3-F	CCTAGCCCTCTTTCCTGGTT	453
Atp5h-ex3-R	GTTGAAGGCAGAGAGCCAAC	
Atp5h-ex4-F	GTGGTGGCCCTTCAGATAAA	409
Atp5h-ex4-R	CTAAAGGCCCTCCAAGTCCT	
Atp5h-ex5-F	GCGGGTCCTGTGTGATTAGT	429
Atp5h-ex5-R	CGTGGTGGCACTTGCTTATA	
Atp5h-ex6-F	TAAGCTGCTTTCCTGCCTGA	383
Atp5h-ex6-R	CAAAGAGCAGAAACCTGTTAGC	
Atp5h-ex7-F	CTGGGACCCATTGTCTCTGT	403

disorders, but elevated C4-OH levels were seen when compared with control mice during normal and fasting conditions. In addition, these abnormal fatty acid profiles in C4-OH mice in independent litters of the same family suggested that this phenotype was heritable. ENU mutagenesis is a powerful method for producing and screening genetic variants for gene function studies in the whole organism. A potential problem is the presence of other mutations induced by ENU, which may confound the observed phenotypes. In our study, we applied a three-generation strategy to detect recessive mutations. We have further bred the affected mice with wild type mice and carried out outcross breeding. All mice, now through the sixth generation, have continued to show a 100% phenotype due to the candidate genes mutation. Other mutations, if present, are likely to be diluted out and contribute little, if any, to the observed phenotypes.

To examine protein expression levels, the first approach we used was one-dimensional SDS-PAGE. However, we did not observe any differential protein bands between ENU control and mutant mice. To increase the amount of protein loading and the resolving power, we then used 2-DE as an alternative method. The principle of 2-DE is based on a different protein isoelectric point and molecular weight to separate a complex group of proteins in cells.[9,12] In our experimental approach, we focused on the upregulated proteins such as myosin light chain 2, myosin light chain 3, myosin light chain 6B, AK1 and ATP5H in the control group, rather than downregulation in C4-OH mice. Short-chain fatty acid oxidation occurs mainly in mitochondria, and therefore, we focused on *Ak1* and *Atp5h* as candidate mutant genes for further nucleotide sequence analysis.

AK1 (EC:2.7.4.3.) catalyzes the reversible transfer of the terminal phosphate group between ATP and adenosine monophosphate and has been shown to be polymorphic in red cells of more than 30 populations.[28] It is located in the intermembrane space of mitochondria and can be used to estimate the extent of *in vivo* hemolysis in hemolytic patients.[29] Mitochondrial membrane ATP synthase (F1F0 ATP synthase or Complex V) produces ATP from ADP in the presence of a proton gradient across the membrane that is generated by electron transport complexes of the respiratory chain.[30] F-type ATPases consist of two structural domains, F_1-containing extramembranous catalytic core and F_0-containing membrane proton channel, linked together by a central stalk and a peripheral stalk. During catalysis, ATP synthesis in the catalytic domain of F_1 is coupled via a rotary mechanism of the central stalk subunits to proton translocation.[31] F-type ATPases have two components that are the CF_1 catalytic core and CF_0 membrane proton channel. CF_0 has nine subunits: a, b, c, d, e, f, g, F6 and A6L.[32] Expression of the mitochondrial ATP synthase beta subunit, ATP5H and mitochondrial ATP synthase beta subunit precursor are increased by a ketogenic diet in the rat.[33] In a clinical study, the sera from patients with human Duchenne (X-linked) progressive muscular dystrophy contained elevated adenylate kinase activity.[34]

In our study, genomic DNA was extracted from both control and C4-OH mice tails, but there was no variation or mutation in *Ak1* and *Atp5h* after full genomic sequencing. Our data suggest that metabolomics-guided screening, coupled with ENU mutagenesis, is a powerful approach for uncovering novel gene mutation for genetic metabolic disorders. This mimicking of C4-OH mice with a fatty acid oxidation disorder, although no mutations were found in both candidate genes, may be due to a limitation of the 2-D technique in resolving very small, very large, or highly basic, acidic, or hydrophobic proteins.[20] However, there are several genome-wide approaches such as quantitative trait linkage analysis that helps narrow down the candidate region and ultimately maps the point mutations responsible for the appearance of these new traits.[35] More sensitive methods such as silver staining and the modified Coomassie Brilliant Blue staining method at nanogram sensitivity compatible with proteomic analysis

also increase differential spots for further protein identification.[36] Additional research is required to further clarify the mechanisms responsible for these effects.

We have characterized the 2-DE map of mitochondrial proteins of the gastrocnemius in mice, and have detected and identified two proteins that were much lower in C4-OH mice compared with controls. Both AK1 and ATP5H were linked to fatty acid metabolism; however, no variation or mutation was found in *Ak1* and *Atp5h* by direct genomic sequencing. The proteomic approach could assist in achieving comprehensive biological profiling rather than genetics alone, as well as determining new candidate genes involved in fatty acid metabolism.

Acknowledgments

This study was supported by research grants from the National Science Council (NSC 93-2311-B-038-005) and Taipei Medical University Hospital (96TMU-TMUH-16), Taiwan. We thank Professor Chen-Pei David Tu, Department of Biochemistry and Molecular Biology, Pennsylvania State University, University Park, for his valuable suggestions during the study.

References

1. Balling R. ENU mutagenesis: analyzing gene function in mice. *Annu Rev Genomics Hum Genet* 2001;2:463–92.
2. Popp RA, Bailiff EG, Skow LC, Johnson FM, Lewis SE. Analysis of a mouse alpha-globin gene mutation induced by ethylnitrosourea. *Genetics* 1983;105:157–67.
3. Russell WL, Kelly EM, Hunsicker PR, Bangham JW, Maddux SC, Phipps EL. Specific-locus test shows ethylnitrosourea to be the most potent mutagen in the mouse. *Proc Natl Acad Sci USA* 1979;76:5818–9.
4. Demidem A, Morvan D, Madelmont JC. Bystander effects are induced by CENU treatment and associated with altered protein secretory activity of treated tumor cells: a relay for chemotherapy? *Int J Cancer* 2006;119:992–1004.
5. Harding CO, Williams P, Pflanzer DM, Colwell RE, Lyne PW, Wolff JA. sar: a genetic mouse model for human sarcosinemia generated by ethylnitrosourea mutagenesis. *Proc Natl Acad Sci USA* 1992;89:2644–8.
6. Justice MJ, Noveroske JK, Weber JS, Zheng B, Bradley A. Mouse ENU mutagenesis. *Hum Mol Genet* 1999;8:1955–63.
7. Shibuya T, Morimoto K. A review of the genotoxicity of 1-ethyl-1-nitrosourea. *Mutat Res* 1993;297:3–38.
8. Yan JX, Harry RA, Wait R, Welson SY, Emery PW, Preedy VR, Dunn MJ. Separation and identification of rat skeletal muscle proteins using two-dimensional gel electrophoresis and mass spectrometry. *Proteomics* 2001;1:424–34.
9. Issaq H, Veenstra T. Two-dimensional polyacrylamide gel electrophoresis (2D-PAGE): advances and perspectives. *Biotechniques* 2008;44:697–8, 700.
10. Hirabayashi T. Two-dimensional gel electrophoresis of chicken skeletal muscle proteins with agarose gels in the first dimension. *Anal Biochem* 1981;117:443–51.
11. Lorkin PA, Lehmann H. Investigation of malignant hyperthermia: analysis of skeletal muscle proteins from normal and halothane sensitive pigs by two dimensional gel electrophoresis. *J Med Genet* 1983;20:18–24.
12. Lombardi A, Silvestri E, Cioffi F, Senese R, Lanni A, Goglia F, de Lange P, et al. Defining the transcriptomic and proteomic profiles of rat ageing skeletal muscle by the use of a cDNA array, 2D- and Blue native-PAGE approach. *J Proteomics* 2009;72:708–21.
13. Sherton CC, Wool IG. A comparison of the proteins of rat skeletal muscle and liver ribosomes by two-dimensional polyacrylamide gel electrophoresis. Observations on the partition of proteins between ribosomal subunits and a description of two acidic proteins in the large subunit. *J Biol Chem* 1974;249:2258–67.
14. Barrett EJ, Headon DR. Two-dimensional polyacrylamide gel electrophoresis of rabbit skeletal muscle microsomal proteins. *FEBS Lett* 1975;51:121–5.
15. Tao Q, Wang Z, Zhao H, Baeyens WR, Delanghe JR, Huang L, Ouyang J, et al. Direct chemiluminescent imaging detection of human serum proteins in two-dimensional polyacrylamide gel electrophoresis. *Proteomics* 2007;7:3481–90.
16. McGregor E, Kempster L, Wait R, Welson SY, Gosling M, Dunn MJ, Powel JT. Identification and mapping of human saphenous vein medial smooth muscle proteins by two-dimensional polyacrylamide gel electrophoresis. *Proteomics* 2001;1:1405–14.
17. Tanaka S, Sakai A, Kimura K, Yoshida H, Fushitani H, Ogata A, Miyamoto A, et al. Proteomic analysis of the basic proteins in 5-fluorouracil resistance of human colon cancer cell line using the radical-free and highly reducing method of two-dimensional polyacrylamide gel electrophoresis. *Int J Oncol* 2008;33:361–70.
18. Dunn MJ. Two-dimensional polyacrylamide gel electrophoresis for cardiovascular proteomics. *Methods Mol Biol* 2007;357:3–13.
19. Jarrold B, DeMuth J, Greis K, Burt T, Wang F. An effective skeletal muscle prefractionation method to remove abundant structural proteins for optimized two-dimensional gel electrophoresis. *Electrophoresis* 2005;26:2269–78.
20. Hobson DJ, Rupa P, Diaz GJ, Zhang H, Yang M, Mine Y, Turner PV, et al. Proteomic analysis of ovomucoid hypersensitivity in mice by two-dimensional difference gel electrophoresis (2D-DIGE). *Food Chem Toxicol* 2007;45:2372–80.
21. Kim JJ, Battaile KP. Burning fat: the structural basis of fatty acid beta-oxidation. *Curr Opin Struct Biol* 2002;12:721–8.
22. Sim KG, Hammond J, Wilcken B. Strategies for the diagnosis of mitochondrial fatty acid beta-oxidation disorders. *Clin Chim Acta* 2002;323:37–58.
23. Wu JY, Kao HJ, Li SC, Stevens R, Hillman S, Millington D, Chen YT. ENU mutagenesis identifies mice with mitochondrial branched-chain aminotransferase deficiency resembling human maple syrup urine disease. *J Clin Invest* 2004;113:434–40.
24. Weber JS, Salinger A, Justice MJ. Optimal N-ethyl-N-nitrosourea (ENU) doses for inbred mouse strains. *Genesis* 2000;26:230–3.
25. Roe CR, Millington DS, Maltby DA, Bohan TP, Kahler SG, Chalmers RA. Diagnostic and therapeutic implications of medium-chain acylcarnitines in the medium-chain acyl-coA dehydrogenase deficiency. *Pediatr Res* 1985;19:459–66.
26. Li SC, Chen CM, Goldstein JL, Wu JY, Lemyre E, Burrow TA, Kang PB, et al. Glycogen storage disease type IV: novel mutations and molecular characterization of a heterogeneous disorder. *J Inherit Metab Dis* 2010 Jan 8. [Epub ahead of print]
27. Mortensen PB, Rasmussen HS, Holtug K. Lactulose detoxifies in vitro short-chain fatty acid production in colonic contents induced by blood: implications for hepatic coma. *Gastroenterology* 1988;94:750–4.
28. Saison R, Giblett ER. 6-phosphogluconic dehydrogenase polymorphism in the pig. *Vox Sang* 1969;16:514–6.
29. Thomas G, Murthy VV. Erythrocyte adenylate kinase isoenzyme as a marker for hemolysis. *J Clin Lab Anal* 1997;11:351–6.
30. Grover GJ, Marone PA, Koetzner L, Seto-Young D. Energetic signalling in the control of mitochondrial F1F0 ATP synthase

activity in health and disease. *Int J Biochem Cell Biol* 2008;40: 2698–701.
31. Fritz M, Muller V. An intermediate step in the evolution of ATPases—the F1F0-ATPase from *Acetobacterium woodii* contains F-type and V-type rotor subunits and is capable of ATP synthesis. *FEBS J* 2007;274:3421–8.
32. Boyer PD. The binding change mechanism for ATP synthase—some probabilities and possibilities. *Biochim Biophys Acta* 1993; 1140:215–50.
33. Noh HS, Lee HP, Kim DW, Kang SS, Cho GJ, Rho JM, Choi WS. A cDNA microarray analysis of gene expression profiles in rat hippocampus following a ketogenic diet. *Brain Res Mol Brain Res* 2004;129:80–7.
34. Hamada M, Okuda H, Oka K, Watanabe T, Ueda K, Nojima M, Kuby SA, et al. An aberrant adenylate kinase isoenzyme from the serum of patients with Duchenne muscular dystrophy. *Biochim Biophys Acta* 1981;660:227–37.
35. Nishimura I, Drake TA, Lusis AJ, Lyons KM, Nadeau JH, Zernik J. ENU large-scale mutagenesis and quantitative trait linkage (QTL) analysis in mice: novel technologies for searching polygenetic determinants of craniofacial abnormalities. *Crit Rev Oral Biol Med* 2003;14:320–30.
36. Wang X, Li X, Li Y. A modified Coomassie Brilliant Blue staining method at nanogram sensitivity compatible with proteomic analysis. *Biotechnol Lett* 2007;29:1599–603.